

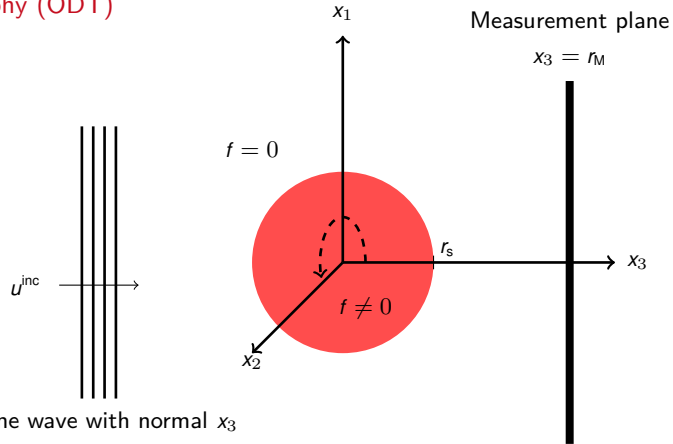


Fourier Reconstruction in Diffraction Tomography of an Irregularly Moving Object

Michael Quellmalz | TU Berlin | SIAM Imaging Science, 21 March 2022

joint work with Robert Beinert, Florian Faucher, Clemens Kirisits, Monika Ritsch-Martel, Otmar Scherzer, Eric Setterqvist, Gabriele Steidl

Optical Diffraction Tomography (ODT)



Incident field: Plane wave with normal x_3



C Kirisits, M Quellmalz, M Ritsch-Martel, O Scherzer, E Setterqvist, G Steidl.

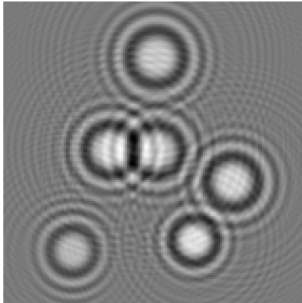
Fourier reconstruction for diffraction tomography of an object rotated into arbitrary orientations.

Inverse Problems 37, 2021.



Optical Diffraction

Optical diffraction occurs when the wavelength of the imaging beam is large
 \approx the size of the object (μm scale)



Simulation of the scattered field from
spherical particles (size \approx wavelength)

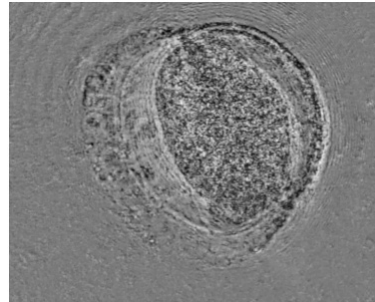


Image with diffraction
© Medizinische Universität Innsbruck

Modeling of Optical Diffraction Tomography

- We have field $u^{\text{tot}}(x_1, x_2, r_M)$ at measurement plane $x_3 = r_M$
- We want scattering potential $f(\mathbf{x})$ with $\text{supp } f \subset \mathcal{B}_{r_s} \subset \mathbb{R}^3$
- Object illuminated by plane wave $u^{\text{inc}}(\mathbf{x}) = e^{ik_0 x_3}$
- Total field $u^{\text{tot}}(\mathbf{r}) = u^{\text{sca}}(\mathbf{r}) + u^{\text{inc}}(\mathbf{r})$ solves the wave equation

$$-(\Delta + f(\mathbf{r}) + k_0^2) u^{\text{tot}}(\mathbf{r}) = 0$$

- Rearranging yields

$$-(\Delta + k_0^2) u^{\text{sca}}(\mathbf{r}) - \underbrace{(\Delta + k_0^2) u^{\text{inc}}(\mathbf{r})}_{=0} = f(\mathbf{r}) (u^{\text{sca}}(\mathbf{r}) + u^{\text{inc}}(\mathbf{r}))$$

Born approximation

Assuming $|u^{\text{sca}}| \ll |u^{\text{inc}}|$, we obtain

$$-(\Delta + k_0^2) u^{\text{sca}}(\mathbf{r}) = f(\mathbf{r}) u^{\text{inc}}(\mathbf{r})$$

Modeling of Optical Diffraction Tomography

- We have field $u^{\text{tot}}(x_1, x_2, r_M)$ at measurement plane $x_3 = r_M$
- We want scattering potential $f(\mathbf{x})$ with $\text{supp } f \subset \mathcal{B}_{r_s} \subset \mathbb{R}^3$
- Object illuminated by plane wave $u^{\text{inc}}(\mathbf{x}) = e^{ik_0 x_3}$
- Total field $u^{\text{tot}}(\mathbf{r}) = u^{\text{sca}}(\mathbf{r}) + u^{\text{inc}}(\mathbf{r})$ solves the wave equation

$$-(\Delta + f(\mathbf{r}) + k_0^2) u^{\text{tot}}(\mathbf{r}) = 0$$

- Rearranging yields

$$-(\Delta + k_0^2) u^{\text{sca}}(\mathbf{r}) - \underbrace{(\Delta + k_0^2) u^{\text{inc}}(\mathbf{r})}_{=0} = f(\mathbf{r}) (u^{\text{sca}}(\mathbf{r}) + u^{\text{inc}}(\mathbf{r}))$$

Born approximation

Assuming $|u^{\text{sca}}| \ll |u^{\text{inc}}|$, we obtain

$$-(\Delta + k_0^2) u^{\text{sca}}(\mathbf{r}) = f(\mathbf{r}) u^{\text{inc}}(\mathbf{r})$$

Modeling of Optical Diffraction Tomography

- We have field $u^{\text{tot}}(x_1, x_2, r_M)$ at measurement plane $x_3 = r_M$
- We want scattering potential $f(\mathbf{x})$ with $\text{supp } f \subset \mathcal{B}_{r_s} \subset \mathbb{R}^3$
- Object illuminated by plane wave $u^{\text{inc}}(\mathbf{x}) = e^{ik_0 x_3}$
- Total field $u^{\text{tot}}(\mathbf{r}) = u^{\text{sca}}(\mathbf{r}) + u^{\text{inc}}(\mathbf{r})$ solves the wave equation

$$- (\Delta + f(\mathbf{r}) + k_0^2) u^{\text{tot}}(\mathbf{r}) = 0$$

- Rearranging yields

$$- (\Delta + k_0^2) u^{\text{sca}}(\mathbf{r}) - \underbrace{(\Delta + k_0^2) u^{\text{inc}}(\mathbf{r})}_{=0} = f(\mathbf{r}) (u^{\text{sca}}(\mathbf{r}) + u^{\text{inc}}(\mathbf{r}))$$

Born approximation

Assuming $|u^{\text{sca}}| \ll |u^{\text{inc}}|$, we obtain

$$- (\Delta + k_0^2) u^{\text{sca}}(\mathbf{r}) = f(\mathbf{r}) u^{\text{inc}}(\mathbf{r})$$

Modeling of Optical Diffraction Tomography

- We have field $u^{\text{tot}}(x_1, x_2, r_M)$ at measurement plane $x_3 = r_M$
- We want scattering potential $f(\mathbf{x})$ with $\text{supp } f \subset \mathcal{B}_{r_s} \subset \mathbb{R}^3$
- Object illuminated by plane wave $u^{\text{inc}}(\mathbf{x}) = e^{ik_0 x_3}$
- Total field $u^{\text{tot}}(\mathbf{r}) = u^{\text{sca}}(\mathbf{r}) + u^{\text{inc}}(\mathbf{r})$ solves the wave equation

$$- (\Delta + f(\mathbf{r}) + k_0^2) u^{\text{tot}}(\mathbf{r}) = 0$$

- Rearranging yields

$$- (\Delta + k_0^2) u^{\text{sca}}(\mathbf{r}) - \underbrace{(\Delta + k_0^2) u^{\text{inc}}(\mathbf{r})}_{=0} = f(\mathbf{r}) (u^{\text{sca}}(\mathbf{r}) + u^{\text{inc}}(\mathbf{r}))$$

Born approximation

Assuming $|u^{\text{sca}}| \ll |u^{\text{inc}}|$, we obtain

$$- (\Delta + k_0^2) u^{\text{sca}}(\mathbf{r}) = f(\mathbf{r}) u^{\text{inc}}(\mathbf{r})$$

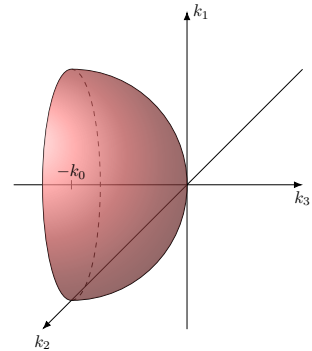
Fourier diffraction theorem [Kirisits Q. Ritsch-Marte Scherzer Settegrqvist Steidl 2021]

1. scattering potential $f \in L^p$, $p > 1$, where $\text{supp}(f) \subset \mathcal{B}_{r_s}$, $0 < r_s < r_M$,
2. incident field is a plane wave $u^{\text{inc}}(\mathbf{x}) = e^{ik_0 x_3}$,
3. Born approximation is valid and u^{sca} satisfies the Sommerfeld condition (u^{sca} is an outgoing wave),
4. scattered field u^{sca} is measured at the plane $r_3 = r_M$.

Then

$$\sqrt{\frac{2}{\pi}} \kappa i e^{-i\kappa r_M} \mathcal{F}_{1,2} \underbrace{u^{\text{sca}}(k_1, k_2, r_M)}_{\text{measurements}} = \mathcal{F}f(\mathbf{h}(k_1, k_2)), \quad (k_1, k_2) \in \mathbb{R}^2,$$

where $\mathbf{h}(k_1, k_2) := \begin{pmatrix} k_1 \\ k_2 \\ \kappa - k_0 \end{pmatrix}$ and $\kappa := \sqrt{k_0^2 - k_1^2 - k_2^2}$.



Semisphere $\mathbf{h}(\mathbf{k})$ of available data in Fourier space

based on [Wolf 1969] [Natterer Wuebbeling 2001] [Kak Slaney 2001]

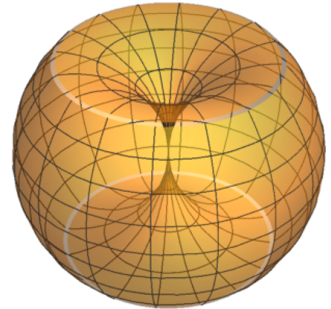
Fourier diffraction theorem (with rotation)

1. scattering potential $f \in L^p$, $p > 1$, where $\text{supp}(f) \subset \mathcal{B}_{r_s}$, $0 < r_s < r_M$,
2. incident field is a plane wave $u^{\text{inc}}(\mathbf{x}) = e^{ik_0 x_3}$,
3. Born approximation is valid and u^{sca} satisfies the Sommerfeld condition (u^{sca} is an outgoing wave),
4. scattered field u^{sca} is measured at the plane $r_3 = r_M$.

Then

$$\sqrt{\frac{2}{\pi}} \kappa i e^{-i\kappa r_M} \mathcal{F}_{1,2} \underbrace{u^{\text{sca}}(k_1, k_2, r_M)}_{\text{measurements}} = \mathcal{F}f(R_t \mathbf{h}(k_1, k_2)), \quad (k_1, k_2) \in \mathbb{R}^2,$$

$$\text{where } \mathbf{h}(k_1, k_2) := \begin{pmatrix} k_1 \\ k_2 \\ \kappa - k_0 \end{pmatrix} \text{ and } \kappa := \sqrt{k_0^2 - k_1^2 - k_2^2}.$$



Set of available Fourier space data for full rotation

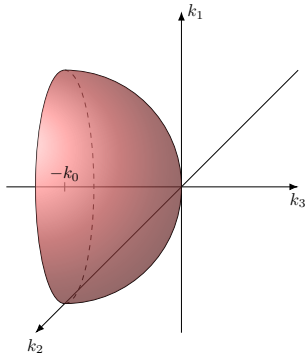
Rotation $R_t \in \text{SO}(3)$ at time $t \in [0, T]$

Comparison with Computerized Tomography

Optical diffraction tomography (ODT)

diffraction of imaging beam

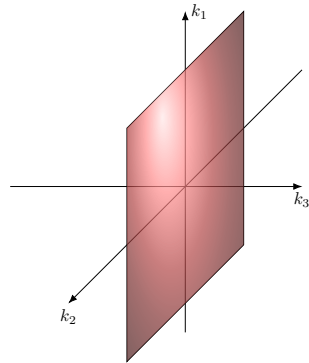
Data: Fourier transform on semispheres containing $\mathbf{0}$



Computerized tomography (CT)

light travels on lines

Data: Fourier transform on planes containing $\mathbf{0}$



Discretization

- Uniform sampling of $f(\mathbf{x}_k = \mathbf{k} \frac{2L_s}{K})$, $\mathbf{k} \in \mathcal{I}_K^3 := \{-K/2, \dots, K/2 - 1\}^3$
- Uniform sampling of measurements $u_{t_m}^{\text{tot}}(\mathbf{y}_n, r_M)$, $\mathbf{y}_n = \mathbf{n} \frac{2L_M}{N}$, $m = 1, \dots, M$, $\mathbf{n} \in \mathcal{I}_N^2$
- **discrete Fourier transform (DFT)**

$$[\mathbf{F}_{\text{DFT}} u_{t_m}^{\text{sca}}]_{\ell} := \sum_{\mathbf{n} \in \mathcal{I}_N^2} u_{t_m}^{\text{sca}}(\mathbf{y}_n, r_M) e^{-2\pi i \mathbf{n} \cdot \ell / N}, \quad \ell \in \mathcal{I}_N^2,$$

- **Non-uniform discrete Fourier transform (NDFT)**

$$[\mathbf{F}_{\text{NDFT}} \mathbf{f}]_{m, \ell} := \sum_{\mathbf{k} \in \mathcal{I}_K^3} f_{\mathbf{k}} e^{-i \mathbf{x}_{\mathbf{k}} \cdot (R_{t_m} h(\mathbf{y}_{\ell}))}, \quad m \in \mathcal{J}_M, \ell \in \mathcal{I}_N^2$$

Discretized forward operator

$$\mathbf{D}^{\text{tot}} \mathbf{f} := \mathbf{F}_{\text{DFT}}^{-1}(\mathbf{c} \odot \mathbf{F}_{\text{NDFT}} \mathbf{f}) + e^{i k_0 r_M}, \quad \mathbf{f} \in \mathbb{R}^{K^d},$$

where $\mathbf{c} = \left[\frac{i}{\kappa(\mathbf{y}_{\ell})} e^{i \kappa(\mathbf{y}_{\ell}) r_M} \left(\frac{N}{L_M}\right)^{d-1} \left(\frac{L_S}{K}\right)^d \right]_{\ell \in \mathcal{I}_N^2}$

Reconstruction algorithm

Input: Scattered wave $\mathbf{v}_{m,n}^{\text{sca}} := u_{t_m}^{\text{tot}}\left(\mathbf{n} \frac{2L_M}{N}, r_M\right) - e^{ik_0 r_M}$, $m \in \mathcal{J}_M$, $\mathbf{n} \in \mathcal{I}_N^{d-1}$.

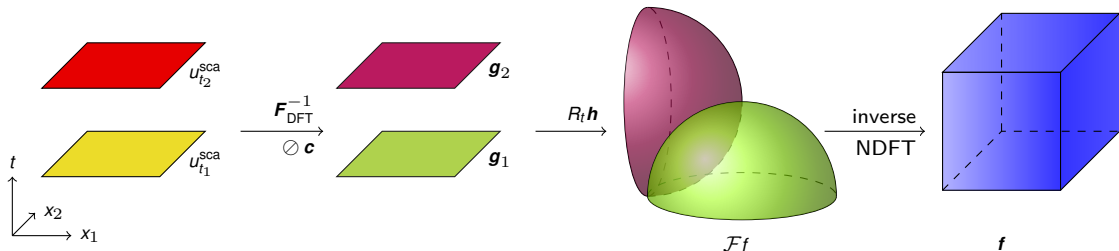
for $m = 1, \dots, M$

$$\tilde{\mathbf{g}}_m := \mathbf{F}_{\text{DFT}} \mathbf{v}_m^{\text{sca}}$$

$$\mathbf{g}_m := \tilde{\mathbf{g}}_m \oslash \mathbf{c}, \text{ where } \oslash \text{ is the Hadamard (entrywise) division}$$

Compute the **inverse NDFT** by solving $\mathbf{F}_{\text{NDFT}} \mathbf{f} = \mathbf{g}$ for \mathbf{f}

Output: Scattering potential $\mathbf{f} \approx [f(\mathbf{x}_k)]_{\mathbf{k} \in \mathcal{I}_k^d}$.



Method 1: Backpropagation

Idea: Compute inverse Fourier transform of $\mathcal{F}f$ restricted to the set of available data \mathcal{Y} :

$$f_{\text{bp}}(\mathbf{x}) := (2\pi)^{-\frac{3}{2}} \int_{\mathcal{Y}} \mathcal{F}f(\mathbf{k}) e^{i\mathbf{k}\cdot\mathbf{x}} d\mathbf{k}.$$

Theorem

[Kirisits, Q, Ritsch-Martel, Scherzer, Setteqvist, Steidl 2021]

Consider the rotation R_t round axis $\mathbf{n} \in C^1([0, T], S^2)$ with angle $\alpha \in C^1[0, T]$. Then

$$f_{\text{bp}}(\mathbf{x}) = (2\pi)^{-\frac{3}{2}} \int_0^T \int_{\mathcal{B}_{k_0}} \mathcal{F}f(R_t \mathbf{h}(k_1, k_2)) e^{iR_t \mathbf{h}(k_1, k_2) \cdot \mathbf{x}} \frac{|\det \nabla T(k_1, k_2, t)|}{\text{Card } T^{-1}(T(k_1, k_2, t))} d(k_1, k_2) dt,$$

where

$$|\det \nabla T(k_1, k_2, t)| = \frac{k_0}{\kappa} \left| \left((1 - \cos \alpha) (n_3 \mathbf{n}' \cdot \mathbf{h} - n_3' \mathbf{n} \cdot \mathbf{h}) - n_3 \mathbf{n} \cdot (\mathbf{n}' \times \mathbf{h}) \sin \alpha \right) - \alpha' (n_1 k_2 - n_2 k_1) + (\mathbf{n} \cdot \mathbf{h}) (n_1 n_2' - n_2 n_1') \sin \alpha \right|,$$

and $T(k_1, k_2, t) := R_t \mathbf{h}(k_1, k_2)$.

It is complicated to determine the Crofton symbol $\text{Card}(T^{-1}(\mathbf{y}))$ algebraically (except for a constant \mathbf{n}).

Method 1: Backpropagation

Idea: Compute inverse Fourier transform of $\mathcal{F}f$ restricted to the set of available data \mathcal{Y} :

$$f_{\text{bp}}(\mathbf{x}) := (2\pi)^{-\frac{3}{2}} \int_{\mathcal{Y}} \mathcal{F}f(\mathbf{k}) e^{i\mathbf{k}\cdot\mathbf{x}} d\mathbf{k}.$$

Theorem

[Kirisits, Q, Ritsch-Marte, Scherzer, Setterqvist, Steidl 2021]

Consider the rotation R_t round axis $\mathbf{n} \in C^1([0, T], \mathbb{S}^2)$ with angle $\alpha \in C^1[0, T]$. Then

$$f_{\text{bp}}(\mathbf{x}) = (2\pi)^{-\frac{3}{2}} \int_0^T \int_{\mathcal{B}_{k_0}} \mathcal{F}f(R_t \mathbf{h}(k_1, k_2)) e^{iR_t \mathbf{h}(k_1, k_2) \cdot \mathbf{x}} \frac{|\det \nabla T(k_1, k_2, t)|}{\text{Card } T^{-1}(T(k_1, k_2, t))} d(k_1, k_2) dt,$$

where

$$|\det \nabla T(k_1, k_2, t)| = \frac{k_0}{\kappa} \left| \left((1 - \cos \alpha) (n_3 \mathbf{n}' \cdot \mathbf{h} - n'_3 \mathbf{n} \cdot \mathbf{h}) - n_3 \mathbf{n} \cdot (\mathbf{n}' \times \mathbf{h}) \sin \alpha \right) - \alpha' (n_1 k_2 - n_2 k_1) + (\mathbf{n} \cdot \mathbf{h}) (n_1 n'_2 - n_2 n'_1) \sin \alpha \right|,$$

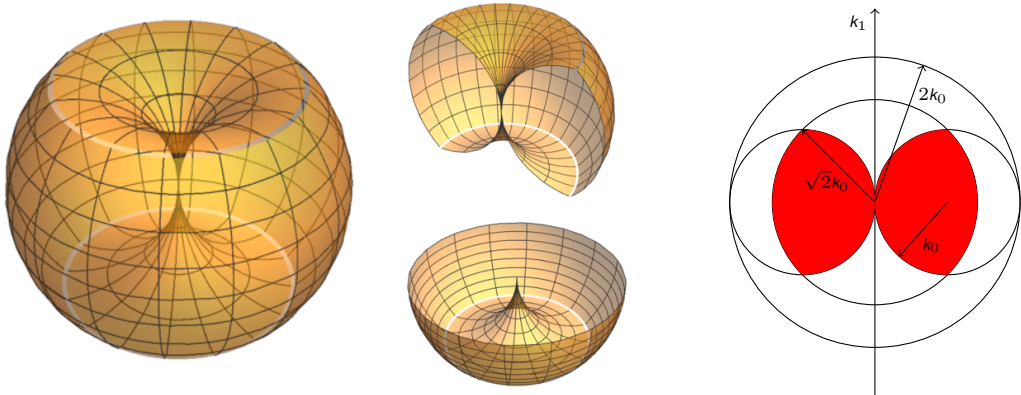
and $T(k_1, k_2, t) := R_t \mathbf{h}(k_1, k_2)$.

It is complicated to determine the Crofton symbol $\text{Card}(T^{-1}(\mathbf{y}))$ algebraically (except for a constant \mathbf{n}).

Example: Rotation Around the First Axis

Backpropagation formula $f_{\text{bp}}(\mathbf{x}) = (2\pi)^{-\frac{3}{2}} \int_0^T \int_{B_{k_0}} \mathcal{F}f(R_t \mathbf{h}(k_1, k_2)) e^{R_t \mathbf{h}(k_1, k_2) \cdot \mathbf{x}} \frac{k_0 |k_2|}{2\kappa} d(k_1, k_2) dt$

[Kak, Slaney 2001] [Müller, Schürmann, Guck 2016]



Approach 2: Conjugate Gradient (CG) Method

- Inversion of the NDFT

- Find a solution $\mathbf{f} \in \mathbb{R}^{K^3}$ of

$$\underset{\mathbf{f} \in \mathbb{R}^{K^d}}{\text{minimize}} \quad \|\mathbf{F}_{\text{NDFT}} \mathbf{f} - \mathbf{g}\|_{2, \mathbf{w}}^2 = \sum_{\mathbf{x}} (\mathbf{F}_{\text{NDFT}} \mathbf{f}(\mathbf{x}) - \mathbf{g}(\mathbf{x}))^2 w(\mathbf{x})$$

- Use Conjugate gradients on the normal equations

Approach 3: TV (Total Variation) Regularization

- Inversion of the NDFT
- Find a solution $\mathbf{f} \in \mathbb{R}^{K^3}$ of

$$\underset{\mathbf{f} \in \mathbb{R}^{K^d}}{\text{minimize}} \quad \chi_{\mathbb{R}_{\geq 0}^{K^d}}(\mathbf{f}) + \frac{1}{2} \|\mathbf{F}_{\text{NDFT}}(\mathbf{f}) - \mathbf{g}\|_{2, \mathbf{w}}^2 + \lambda \text{TV}(\mathbf{f}),$$

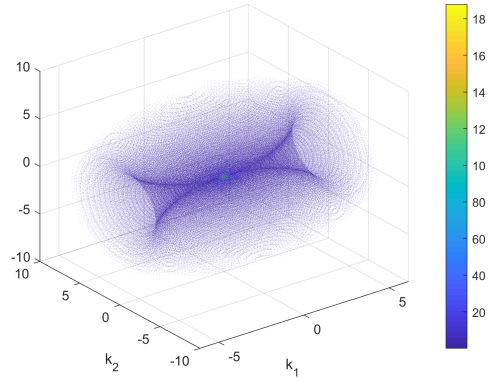
with the **total variation**

$$\text{TV}(\mathbf{f}) := \sum_{\mathbf{k} \in \mathcal{I}_K^3} \|\text{grad } \mathbf{f}(\mathbf{x}_{\mathbf{k}})\|_2$$

- Solve with primal-dual (PD) iteration [Chambolle & Pock 2010]
- Adaptive selection of step sizes [Yokota & Hontani 2017]

Test Setup

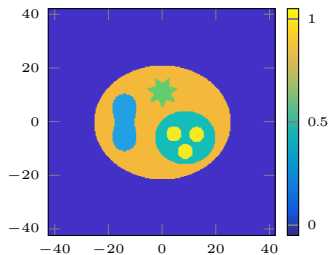
- Normalized wavelength $\lambda = 1 \Rightarrow k_0 = \frac{2\pi}{\lambda} = 2\pi$
- Test function f given analytically
- Generate simulated data via direct convolution with the Green function (also based on Born approximation) to avoid the “inverse crime”
- “missing cones” around the axis of rotation
- **NFFT** (Non-uniform fast Fourier transform): for computing $\mathbf{F}_{\text{NFFT}} \mathbf{f}$ in $\mathcal{O}(N^3 \log N)$ steps
[Dutt Rokhlin 93], [Beylkin 95], [Potts Steidl Tasche 01], [Potts Kunis Keiner 04+]



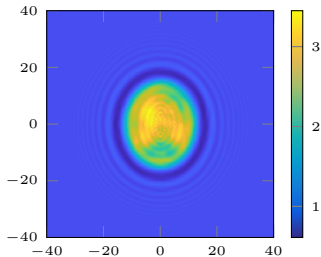
Simulated data: Fourier transform $|\mathcal{F}f|$ at 496944 nodes (constant rotation axis)



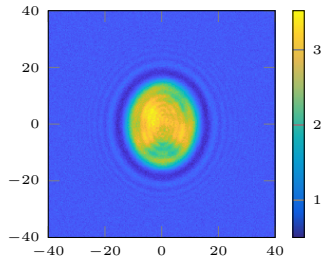
Test data



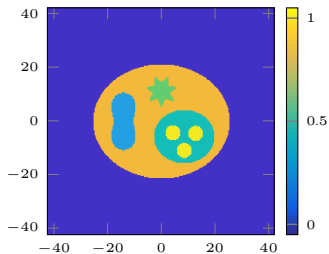
Ground truth f
($240 \times 240 \times 240$ grid)
Slice at $x_3 = 0.35$



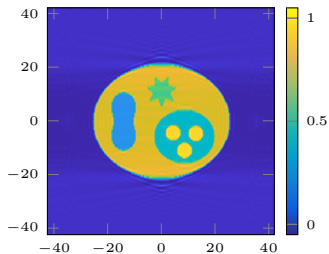
Exact data $|u_t^{\text{tot}}(\cdot, r_M)|$
(240×240 grid and 240 rotations)



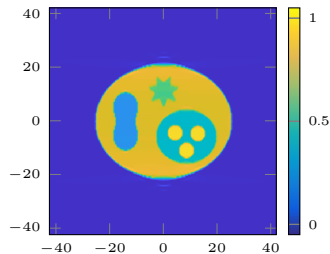
Data with 5% Gaussian noise



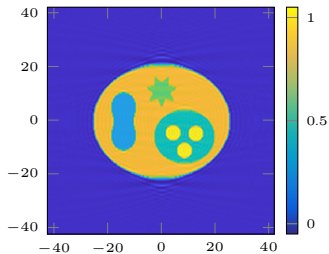
(a) Ground truth f



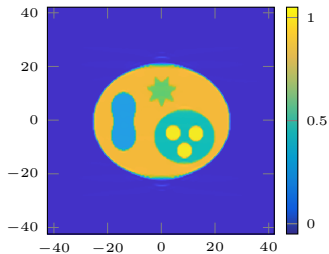
(b) Backpropagation
PSNR 29.07, SSIM 0.614
4 sec



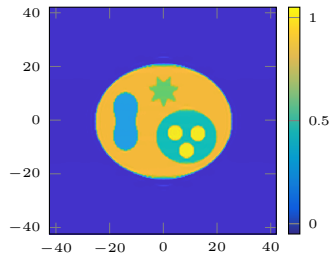
(c) Backprop. and TVdenoise ($\lambda = 0.02$)
PSNR 32.79, SSIM 0.987
37 sec



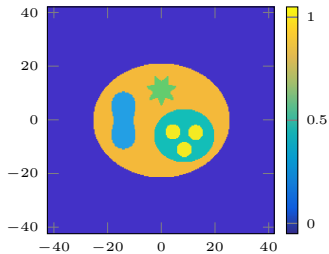
(d) CG Reconstruction
PSNR 33.36, SSIM 0.955
79 sec



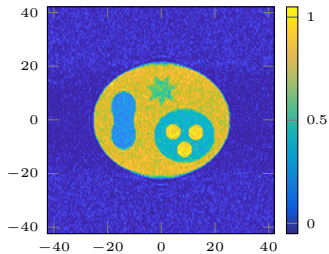
(e) CG and TVdenoise ($\lambda = 0.02$)
PSNR 33.82, SSIM 0.988
31 sec



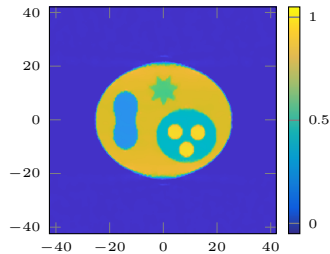
(f) PD with TV ($\lambda = 0.02$)
PSNR 34.36, SSIM 0.957
21 min



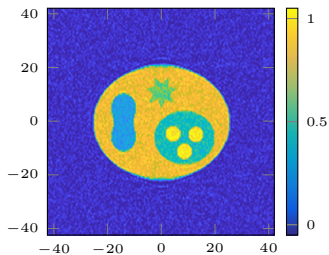
(a) Ground truth f



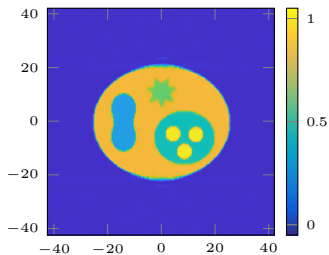
(b) Backpropagation
PSNR 24.53, SSIM 0.178



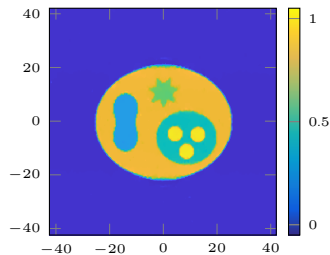
(c) Backpropagation and TVdenoise
($\lambda = 0.05$)
PSNR 32.51, SSIM 0.968



(d) CG Reconstruction
PSNR 26.74, SSIM 0.309

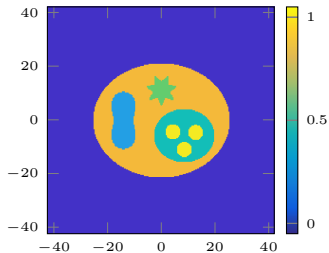


(e) CG and TVdenoise ($\lambda = 0.02$)
PSNR 33.53, SSIM 0.965

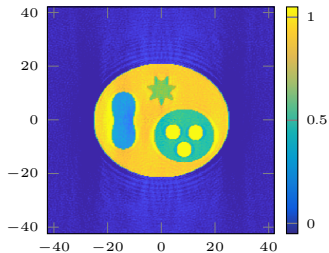


(f) PD with TV ($\lambda = 0.02$)
PSNR 33.58, SSIM 0.736

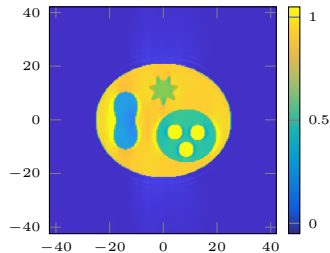
Figure: Slice of 3D reconstruction with 5% Gaussian noise (grid $240 \times 240 \times 240$)



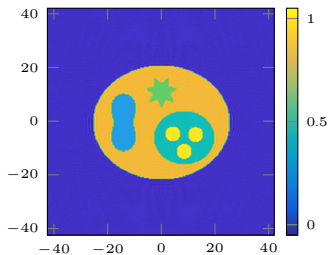
(a) Ground truth f



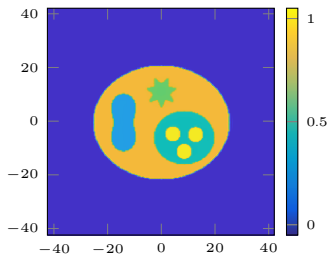
(b) Backpropagation
PSNR 24.17, SSIM 0.171



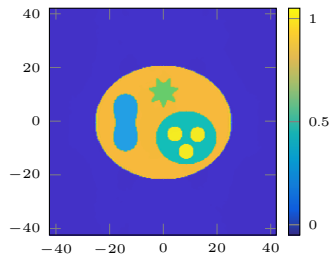
(c) Backpropagation and TVdenoise
($\lambda = 0.02$)
PSNR 29.17, SSIM 0.783



(d) CG Reconstruction
PSNR 35.84, SSIM 0.962



(e) CG and TVdenoise ($\lambda = 0.02$)
PSNR 36.88, SSIM 0.995



(f) PD with TV ($\lambda = 0.02$)
PSNR 40.95, SSIM 0.972

Figure: Slice of 3D reconstruction from exact data with moving rotation axis (grid $240 \times 240 \times 240$)

Phase Retrieval

[Beinert & Q. 2022]

- In practice, one can often measure only the **intensity**

$$|u_t^{\text{tot}}(\mathbf{y}, r_M)| = |u_t^{\text{sca}}(\mathbf{y}, r_M) + e^{ik_0 r_M}|, \quad \mathbf{y} \in \mathbb{R}^2, t \in [0, T]$$

- Existing phase retrieval methods in diffraction tomography
 - require more measurements [Gbur & Wolf 2002] [Wedberg & Stamnes 1995]
 - use far zone approximations [Cheng & Han 2001] [Gureyev & Davis 2004]
 - Consider phase retrieval separate from reconstruction [Maleki & Devaney 1993]
 - Use techniques of ptychography [Horstmeyer Chung Ou Zheng & Yang 2016]
- We require additional information:
 - $f \geq 0$
 - f has bounded support
 - total variation of f

All-at-Once Approach for Phase Retrieval

Forward operator $Df(t, \mathbf{y}) = u_t^{\text{tot}}(\mathbf{y}, r_M)$

Hybrid input-output (HIO) algorithm

[Fienup 1982]

Input: Data $\mathbf{d} = |\mathbf{D}(\mathbf{f})| = |u^{\text{tot}}|$, parameter $\beta \in [0, 1]$, support radius $r_s > 0$.

Initialize $\mathbf{g}^{(0)} := \mathbf{d}$

for $j = 0, 1, 2, \dots$

$$\mathbf{f}^{(j)} := \mathbf{D}^{-1} \mathbf{g}^{(j)}$$

$$\tilde{\mathbf{f}}_k^{(j)} := \begin{cases} \max\{f^{(j)}(\mathbf{x}_k), 0\}, & \|\mathbf{x}_k\|_2 \leq r_s, \\ 0, & \|\mathbf{x}_k\|_2 > r_s, \end{cases}$$

$$f^{(j+1/2)}(\mathbf{x}_k) := \begin{cases} f^{(j)}(\mathbf{x}_k), & \text{if } f^{(j)}(\mathbf{x}_k) = \tilde{\mathbf{f}}^{(j)}(\mathbf{x}_k) \\ f^{(j-1/2)}(\mathbf{x}_k) - \beta(f^{(j)}(\mathbf{x}_k) - \tilde{\mathbf{f}}^{(j)}(\mathbf{x}_k)), & \text{otherwise,} \end{cases}$$

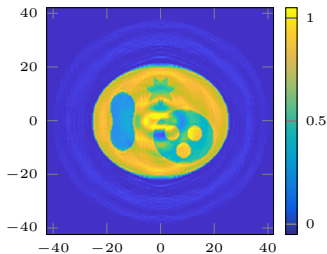
$$\mathbf{g}^{(j+1/2)} := \mathbf{D} \mathbf{f}^{(j+1/2)}$$

$$\mathbf{g}^{(j+1)} := \mathbf{d} \operatorname{sgn}(\mathbf{g}^{(j+1/2)})$$

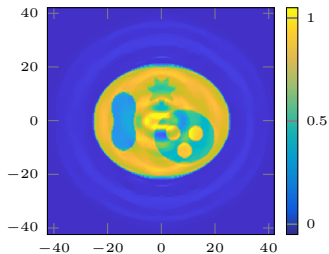
Output: Approximate scattering potential $\mathbf{f}^{(j)}$.



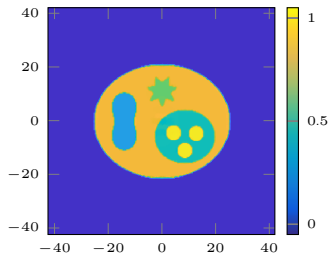
Numerical Phase Retrieval (Exact Data)



(a) HIO/CG reconstruction
 $J_{\text{IO}} = 10$, $J_{\text{CG}} = 5$
PSNR 29.52, SSIM 0.713
5 min



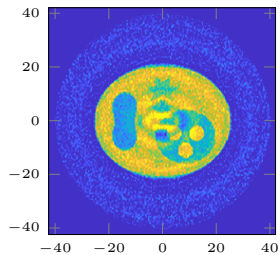
(b) HIO/CG and TVdenoise
 $\lambda = 0.02$, $J_{\text{TV}} = 20$
PSNR 29.88, SSIM 0.713
31 sec



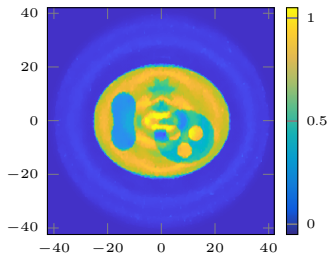
(c) HIO/PD with TV
 $\lambda = 0.01$, $J_{\text{IO}} = 200$, $J_{\text{PD}} = 5$
PSNR 34.92, SSIM 0.994
3 h 48 min

Figure: Slice of 3D HIO phase retrieval

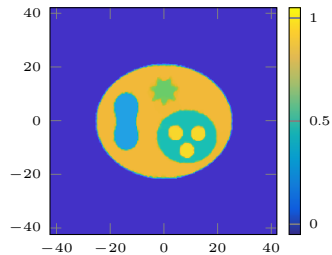
Numerical phase retrieval (noisy data)



(a) HIO/CG reconstruction
 $J_{\text{IO}} = 10$, $J_{\text{CG}} = 5$
 PSNR 24.71, SSIM 0.589



(b) HIO/CG and TVd
 $\lambda = 0.05$, $J_{\text{PD}} = 20$
 PSNR 27.16, SSIM 0.623



(c) HIO/PD with TV
 $\lambda = 0.05$, $J_{\text{IO}} = 200$, $J_{\text{PD}} = 5$
 PSNR 34.10, SSIM 0.993

Figure: Slice of 3D HIO phase retrieval with 5% Gaussian noise



Computational complexity

- Outer loop with HIO and inner loop with primal-dual (PD)
- Both algorithms often show slow convergence
- **Improvements:**
 - Restart the primal dual with the parameters dual variable from the previous outer step
 - Use faster HIO/CG to obtain a starting solution for primal-dual
 - Use fast FFT and NFFT algorithms for the Fourier step
 - Employ the weights from the backpropagation to the minimization problem

Code available on Github: <https://github.com/michaelquellmalz/FourierODT>

Conclusion

- Fourier diffraction theorem on $L^p(\mathcal{B}_{r_s})$, $p > 1$
- Backpropagation formula for arbitrary rotations
- Compared reconstruction method
 - Backpropagation is faster
 - Inverse NFFT is always applicable and shows slightly better results
- Phase retrieval works well with all-at-once HIO and TV regularization

Future research

- Detection of rotation from data
- Application to real-world data

Thank you for your attention!

Conclusion

- Fourier diffraction theorem on $L^p(\mathcal{B}_{r_s})$, $p > 1$
- Backpropagation formula for arbitrary rotations
- Compared reconstruction method
 - Backpropagation is faster
 - Inverse NFFT is always applicable and shows slightly better results
- Phase retrieval works well with all-at-once HIO and TV regularization

Future research

- Detection of rotation from data
- Application to real-world data

Thank you for your attention!

Conclusion

- Fourier diffraction theorem on $L^p(\mathcal{B}_{r_s})$, $p > 1$
- Backpropagation formula for arbitrary rotations
- Compared reconstruction method
 - Backpropagation is faster
 - Inverse NFFT is always applicable and shows slightly better results
- Phase retrieval works well with all-at-once HIO and TV regularization

Future research

- Detection of rotation from data
- Application to real-world data

Thank you for your attention!